Journal of Molecular Liquids 306 (2020) 112909

Contents lists available at ScienceDirect

Journal of Molecular Liquids

journal homepage: www.elsevier.com/locate/molliq

Interfacial water controls the process of adsorption of hyperactive antifreeze proteins onto the ice surface

Joanna Grabowska, Anna Kuffel, Jan Zielkiewicz *

Gdańsk University of Technology, Faculty of Chemistry, Department of Physical Chemistry, Narutowicza 11/12, 80–233 Gdańsk, Poland

ARTICLE INFO

Article history:
Received 29 January 2020
Received in revised form 11 March 2020
Accepted 13 March 2020
Available online 14 March 2020

Keywords:
Solvation water
Structure of water
Protein-ice interaction
Molecular dynamics

ABSTRACT

A mechanism of interactions between the ice-binding surface of a hyperactive antifreeze protein molecule and the ice surface is proposed, involving the influence of water present between the two surfaces on the behavior of the approaching molecule. It is demonstrated that the interfacial water, even before its full solidification, can act as a factor that pushes away or pulls nearer the protein molecule to ensure its proper positioning. It is possible thanks to the structural properties of interfacial water. These properties include the ability to create high-volume aggregates of water molecules. They can appear near and be anchored to both the ice-binding plane of the antifreeze molecule and the ice surface. When an AFP approaches the growing face of ice, these high-volume, ordered structures near the ice and near the AFP molecule merge together smoothly, but only if the proper distance between the ice and the AFP is ensured. If this is not the case, the resulting merged structure is deformed from its preferred shape and as a result a force occurs that attempts to correct the positioning of the protein. Only then the crystallization of the merged aggregate can proceed unhampered which results in binding of the AFP molecule onto the ice.

1. Introduction

Antifreeze proteins (AFPs) can be found in bodily fluids of organisms exposed to temperatures below 0 °C. Their task is to prevent the growth of ice crystals which they fulfill by adsorbing onto the ice surface. Given the level of activity AFPs can be ascribed into one of the two classes: moderately active or hyperactive. The reason for the difference in the activity is thought to be the ability to bind onto the basal plane of ice [1]. Various AFPs differ in shape and size, however, it is believed that the general mechanism of action of AFPs is ultimately the same. When AFP molecules are adsorbed at the ice surface, the further growth of ice can only occur in places where the proteins are not present. Because of that, the interface of this new ice is locally curved. According to the Gibbs-Thomson effect, the melting temperature at a convex surface is lower than at a plane, which eventually stops the formation of ice in a certain range of temperatures. This model requires for an AFP molecule to be irreversibly bound with ice which has been confirmed experimentally [2,3]. However, the whole process is not as straightforward as depicted above and there are still some details that require clarification.

Firstly, the surface of the ice is not sharply defined. At the interface, there is a transient region, which properties extend from almost crystal-like to almost bulk liquid-like. The temperature-dependent thickness of this region is equal to about 1 nm [4–6]. Secondly, it is unclear how an AFP molecule effectively recognizes ice and binds to it in abundance of liquid water in its surroundings [7].

Wierzbicki et al. [8] suggested that an AFP molecule locates itself in the ice/water interfacial region. They proposed that the ice stops growing because the protein "poisons" this interfacial region. Garnham et al. [9], on the other hand, suggested that water molecules closest to the ice-binding surface of an AFP molecule are arranged in a way that very closely resembles the arrangement of water molecules in ice and that the protein attaches to the ice surface through these molecules.

The increased ordering of water at the ice binding surfaces of hyperactive and moderately active antifreeze proteins (relatively to bulk water, as well as to the rest of the protein) was described by many authors [10–14]. These results support the view that the structural properties of solvation water of antifreeze proteins are important to the recognition of the ice and to the adsorption to it. The overwhelming opinion is that the structure of this water resembles ice in some regards [15–20], although this is recently being put into question [21].

In our recent papers [12,22], we also discussed the importance of water for the mechanism of action of antifreeze proteins. We demonstrated that a molecule of a hyperactive *Cf*AFP (from *Choristoneura fumiferana*) is able to perceive the presence of the ice from a distance (about 1 nm), thanks to the properties of interfacial water between the molecule and the ice. This water can be perceived as a kind of glue, connecting the ice and the protein. Hence, our view joins together the concepts of Wierzbicki et al. and Garnham et al. We discovered that

* Corresponding author.
E-mail addresses: joanna.grabowska@pg.edu.pl (J. Grabowska), anna.kuffel@pg.edu.pl (A. Kuffel), jan.zielkiewicz@pg.edu.pl (J. Zielkiewicz).

https://doi.org/10.1016/j.molliq.2020.112909

the position of a properly placed *Cf*AFP molecule is, on average, stabilized relatively to the ice (distance-wise and orientation-wise). We hypothesized [22] that these effects may originate from the fact that in water high-volume, ordered structures can be created, but their unhindered formation in interfacial water requires proper positioning of the *Cf*AFP molecule relatively to the ice. The creation of these structures, immersed in low-volume, disordered structures is anticipated in a model of liquid water that explains many unusual properties of water, proposed by Tanaka [23–26].

In this article, we attempt to extend and justify the concepts that have been evoked by us previously [22], regarding the role of solvation water in the adsorption of the CfAFP molecule onto the ice surface. The direct interactions between the ice and the AFP molecule has already been described by other authors [27], however the early stages of the adsorption, when the molecule and the ice are still separated by solvation water, has not been studied extensively. This is why we concentrate on the role of interfacial water and water-mediated interactions between the ice and the protein. The proposed mechanism takes into account unusual properties of liquid water when compared with other liquids.

2. Materials and methods

2.1. Simulation procedure and system setup

The results were obtained using computer simulations. They were carried out with the molecular dynamics package Amber12 [28] and ff03 force field, suitable for proteins [29]. We used TIP4P/Ice water model [30]. Its freezing temperature, 272 K, is very close to the experimental value. According to the authors, this model "greatly improves the melting properties of previous potentials. But, contrary to the case of TIP5P, the improvement in the melting properties is done without deteriorating the other computed quantities" [30].

The system discussed in this paper consisted of an almost cubic block of hexagonal ice, with the edge length equal to approximately 45 Å. The six planes of the block were the following crystallographic planes of ice: two *basal*, two *primary prism*, two *secondary prism*. Next to the *basal* and *primary prism* planes of the ice block, *Cf*AFP molecules were present (see Fig. 1a). The coordinates of the protein were taken from Protein Data Bank (PDB ID: 1L0S [31]). The composition of the studied system was a consequence of our previous studies. We analyzed the process of freezing at various crystallographic planes of ice, using a very similar ice block [32] and subsequently we studied systems with CfAFP molecules near the faces of the ice block [12,22].

Originally, 120 different, independent copies of the system were prepared. They differed in terms of orientations of water molecules in the ice block, and also, slightly, in terms of positions and orientations of protein molecules relatively to the ice surface (there was a short period of equilibration when proteins were allowed to move freely). Detailed description of the setup of the systems can be found in our previous papers [12,22].

From these 120 systems, 360 new systems were constructed by moving some of the proteins next to the *basal* and *primary prism* planes closer to the ice - to investigate wide range of protein distances from the ice. To achieve this, the coordinates of the proteins initially located at about 1.1 nm from the ice surface, were shifted by 0.2, 0.3 and 0.4 nm towards the ice surface and saved in reference files. These were subsequently used in simulations (280 K, 1 bar), during which the positions of the backbone atoms (except from the oxygen atoms) of the proteins were restrained with harmonic force constant equal to 0.05 kJ/(mol·A^2) for 100 ps and harmonic force constant equal to 0.1 kJ/(mol·A^2) for about 1.3 ns. That resulted in the displacement of the proteins and in bringing them closer to the ice. The histograms of the distances of the protein surfaces to the *basal* and *primary prism* ice planes at the end of this step are given in Fig. 1c.

These preliminary steps were followed by the main simulations of the systems, which were carried out at 250 K and 1 bar. All of the oxygen atoms of the ice block were restrained using force constant equal to 2 kJ/(mol·A^2). The simulation time was 12 ns. The choice of the temperature was guided by our previous studies – the simulations of a very similar ice block [32] demonstrated that at 250 K the crystallization at the faces of the ice block proceeded smoothly and effectively, in the time scale equal to dozens of nanosecond, which is fast enough to study it by simulations.

2.2. Measurements of the force

To measure the force acting on the *Cf*AFP molecule, one atom at the ice-binding surface was selected (CB from THR 36, see Fig. 1a) and restrained during the simulations at a reference point $\vec{r_0} = [r_{x0}, r_{y0}, r_{z0}]$ (coordinates at the start of the simulation at 250 K) using harmonic potential, with the value of the force constant equal to 10 kJ/(mol·A^2). The formula to calculate the force $\vec{F}$ at this selected point $\vec{r_0}$ can be found in

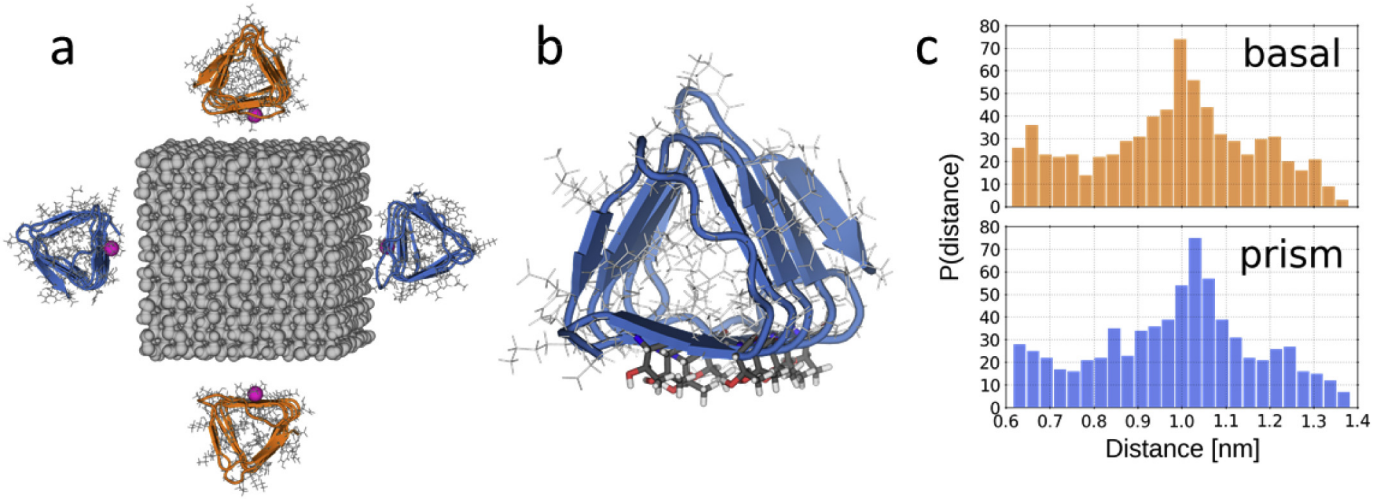

Fig. 1. a) The simulated system – the ice block and the four *Cf*AFP molecules. Atoms restrained to measure the force are marked as spheres. All of the side chains of the protein molecules are shown as gray lines. b) The molecule of CfAFP. The side chains of the nine threonines that build the active site of the protein are presented as sticks. c) The histograms of the distances of the protein surfaces to the *basal* and *primary prism* ice planes. The distance between the protein and the ice was measured as a distance between the geometric mean of the nine oxygen atoms of the threonine residues at the ice-binding surface and the surface of the underlying ice block. Fig. 1a and b were generated with the use of PyMOL [33].

Hwang et al. [34]:

$$F_i = \langle r_i - r_{i0} \rangle \frac{k_B T}{\left\langle (r_i - r_{i0})^2 \right\rangle - \langle r_i - r_{i0} \rangle^2}, i = x, y, z$$

The $\vec{r_0}$ symbol stands for the reference coordinates of the selected and restrained protein atom, $\vec{r}$ stands for the actual coordinates of the atom, T is the temperature, and k_B is the Boltzmann constant. As it follows from this equation, to calculate the force from the trajectory of the system, we measure the fluctuations around the reference point.

3. Results and discussion

The discussion is divided into two main parts. At first, we present the measured values of the force that acts on a *Cf*AFP molecule in the vicinity of the ice surface, as a function of the distance of the ice-binding surface from the ice surface. From these data, the free energy profile is obtained. The second part is devoted to the analysis of the structure of solvation water, located between the *Cf*AFP molecule and the ice surface. This analysis is also performed as a function of the distance between the protein molecule and the ice surface and the results are related to the obtained free energy profile. Based on these data, the molecular mechanism of the adsorption of the *Cf*AFP molecule to the ice surface is proposed, starting from the early stages, when the interfacial water is not yet crystallized.

3.1. The distance-dependent average force acting on an AFP molecule in the vicinity of the ice surface and the accompanying free energy profile

If the *Cf*AFP molecule is not placed at a proper distance from the ice, a force is exerted on the molecule: pulling it closer or pushing it away. We demonstrate that by calculating the force for protein molecules placed at various distances from the ice (720 molecules next to the *basal* plane and 720 next to the *primary prism* plane), as described in Methods. Fig. 2 depicts the averaged components of the vector of the force perpendicular to the ice surface, and the averages were obtained with 0.05 nm interval (the distance between the protein and the ice was measured as a distance between the geometric mean of the nine oxygen atoms of the threonine residues at the ice-binding surface and the surface of the underlying ice block). The positive values represent the force pushing the molecule away, while the negative – pulling it closer to the ice. The order of magnitude of the force is 10^2 pN. It is

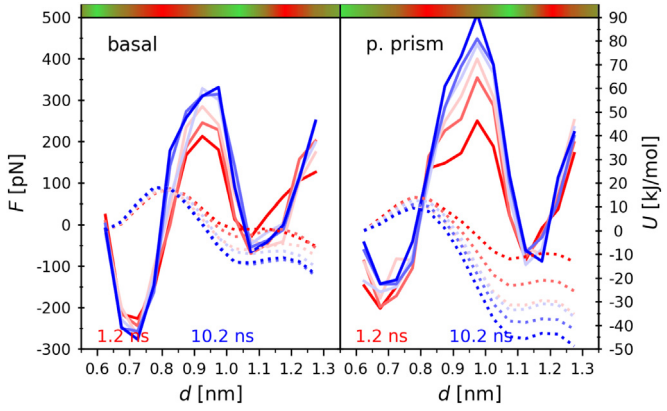

Fig. 2. The average force acting on a *Cf*AFP molecule at various distances from the *basal* and *primary prism* planes of ice (solid line) and the corresponding free energy profile (dashed line). The color scale red-blue illustrates changes in time (red line corresponds to the time 1.2 ns from the start of the simulation, while the darkest blue line – at the end of the simulation; time interval between plots is constant and equal to 1.8 ns). The red-green color bars placed on top of the figure indicate the approximate locations of the minima and maxima of the energy profiles.

reasonable to ask what would be the effect of that force acting on a *Cf*AFP molecule. In the work of Kuffel and Szałachowska [35] it was shown that even relatively small force (several dozens of pN) can displace a protein larger than CfAFP at a significant rate. Furthermore, such a force at 250 K is able to displace a *Cf*AFP molecule with a speed that we estimate to be about 0.01 nm/ns, as can be inferred from our previous results, concerning the protein being pushed away from the ice when oriented with its non-ice-binding surface to the ice [12,22]. Since the force is proportional to the gradient of the free energy of interaction in the system *Cf*AFP molecule – solvation water – the ice surface, we can estimate the shape of the free energy profile. Within the investigated distance range there are two maxima, at about 0.80÷0.85 nm and at about 1.15÷1.20 nm. We also observe a minimum, at about 1.05÷1.10 nm. The results also suggest the presence of another minimum, closer to the ice, possibly at about 0.6 nm. The placing of the protein molecules in the 1.05÷1.10 nm minimum was responsible for the stabilization of the distance of the AFP molecule from the ice observed by us previously [12]. The shape of this free energy function illustrates that the adsorption of the *Cf*AFP molecule does not have to occur via direct interactions with the ice but the molecule can position itself at a certain distance from the ice, which, as we discuss below, is followed by the solidification of the interfacial water.

These results can be compared to the observations made by Mochizuki and Matsumoto [36]. They investigated a different process - the interactions between two *Ri*AFP molecules (in water, at 300 K). *Ri*AFP is a hyperactive antifreeze protein which active site has a structure similar to that of *Cf*AFP. The molecules were facing each other with their ice-binding surfaces. The authors obtained similarly shaped energy profile, including the 0.35 nm distance between the maxima. This is not a coincidence, because the underlying mechanism is, in our opinion, essentially the same – in spite of the fact that the active sites of *Ri*AFP and *Cf*AFP differ in size. In both cases, structural properties of interfacial water should be hold responsible for the shapes of the distributions, what we discuss below.

We can also compare our results with the results obtained by Hudait et al. [27], concerning an AFP molecule in a fully adsorbed state (at a flat ice surface or at a top of a pillar of ice). The energy of binding measured for these adsorbed proteins were equal to about several dozens of kJ/mol. In our opinion, the fact that there are differences between their and our results is understandable, because the effects discussed by us concern a different system – a protein that is not yet fully adsorbed. There is still unsolidified water at the interface. In this context, most significant curves are the ones at the beginning of the simulations, at 1.2 ns and shortly after (red lines in Fig. 2). As early as that, we can see the start of formation of the distant minimum at about 1.1 nm, preceded and followed by maxima. As the simulation proceeds, the depth of the minimum increases as a result of the ongoing solidification of the interfacial water. It is known that the freezing at the *prism* plane is faster than at the *basal* plane [37,38] and because of that the picture changes more profoundly in the case of the protein next to the *primary prism* plane than next to the *basal* plane in the analyzed time span.

The shape of the functions from Fig. 2 can be explained with regard to the specific structural properties of water. Previously [22], we tentatively proposed a mechanism responsible for the pushing of a *Cf*AFP molecule away from the ice when improperly placed. Below, we are going to support that hypothesis and extend the discussion by analyzing the wide range of distances and attempting to investigate the effect not only qualitatively but also quantitatively. Moreover, we now account not only for the possibility of pushing away the *Cf*AFP molecule but also for its pulling towards the ice. This approach emphasizes an important role of solvation water in adsorption process.

3.2. The structure of the solvation water next to the ice-binding AFP surface

The layer of water between the *Cf*AFP molecule and ice is, naturally, strongly heterogeneous. This poses understandable challenges in every

attempt to characterize its structure. Moreover, prior to the solidification, the structure of water, of course, should not be understood in crystallographic terms. It should rather be perceived as a tendency to arrange (fleetingly) the molecules in a specific manner more or less often. Numerous parameters have been proposed to describe the structure of water, such as radial distribution function, tetrahedrality [39], LSI [40,41], Steinhardt parameters [42,43] and many other. None of the above fully describes the complexity of liquid water [44]. We chose the parameters used by us previously in the form of so called ordering maps [20,45], originally proposed by Truskett et al. [46] and developed by Esposito et al. [47] The coordinates of each point on the map represent two different contributions to the entropy of water originating from two-particle correlations: translational (s_{tra} parameter) and orientational (s_{conf} parameter). These parameters should not be identified with the entropy of water - more detailed description can be found in the Supporting Information.

Selection of the appropriate parameter is not the only problem in characterizing the structure of water. Most parameters do not work properly when applied to water molecules that are not surrounded by other water molecules but are next to the protein atoms. In an attempt to overcome this difficulty, we proposed [20,45] to calculate the coordinates of the points on the ordering map for fictitious solvation shells – of the same shape as the solvation shell in question, but artificially filled with bulk water (its coordinates were taken from a separate simulation of water at the same temperature). Finally, we calculated the difference between the parameter obtained for the true solvation water and the fictitious solvation shell. As a result, we hope to estimate how much the structure of solvation water differs (in a given regard) from the bulk water. The definition of the analyzed solvation layer can be found in Supporting Information.

We analyzed the structure of water as a function of two variables: the distance between the protein molecule and the ice surface and the simulation time (Fig. 3). The coordinates of the points on the ordering maps are given by the equations: $\Delta s_{tra} = (s_{tra})_{solv} - (s_{tra})_{bulk}$ and $\Delta s_{conf} = (s_{conf})_{solv} - (s_{conf})_{bulk}$. The data in Fig. 3a depicts the temporal changes in the values of these parameters. With time, the values become more negative, which implies the increase of the local ordering of water as a result of the ongoing freezing.

When the distance is close to the one that corresponds to the second free energy minimum, the process of freezing occurs with the highest rate (the values of Δs_{tra} and Δs_{conf} become increasingly negative the fastest). In the case of the first minimum, the slowed down diffusion is probably responsible for smaller rate of changes. When we move away from the minimum, the rate of the structural changes diminishes. Also, at minima there are some differences in the positions of the points describing the ordering of water near the protein when it is placed next to the *basal* and *primary prism* crystallographic planes, suggesting slightly different mechanisms of rearrangement of water molecules during the crystallization of the interfacial water and implying some plasticity of the solvation layer of the protein.

The structural order parameter as such does not provide much information on the nature of the ordering – on the microscopic structure of water. To gain more insight, we can supplement these results with some parameters characterizing selected properties of hydrogen bonds, such as their energy and geometry (Fig. 2b and c). In the distributions of the values of these parameters, we can see similar cyclic changes (with the distance from the ice) as in the case of the ordering maps. For example, near the minimum at about 1 nm, the energy of hydrogen bonds increases and their network becomes more tetrahedral. Moreover, the highest force that is exerted on the *Cf*AFP molecule, observed for distances slightly above 0.9 nm, is matched with the smallest differences between the solvation water and bulk water – the network of hydrogen bonds is less tetrahedral than at other distances. We could speculate that this water behaves a little as if it was under higher pressure – it attempts to decompress against the protein molecule that is placed too close. At the same time in the values of the measured parameters we do not see the evidence for the solvation water to be more distorted than bulk water (at the same temperature).

The uphill trend (the increase of the energy when the distance diminishes from about 1.1 nm to about 0.8 nm) may seem surprising at first glance but it is understandable in the light of our previous results [22]. To diminish the distance between the protein and the ice, some water molecules from the interfacial region needs to be expelled to the bulk. The energy of interactions of water molecules with their nearest surrounding was found to be more negative in this region than in the bulk [22], hence the increase in the energy. This might bring to mind the concept that AFP, upon approaching the ice, locates itself in the interfacial region, as described by Wierzbicki et al. [8], although direct comparison with our results might be problematic because of differences in the shapes, sizes and amino acid compositions of the studied proteins. This result also resonates with the postulates that the adsorption is in fact achieved by solidification of solvation water of the protein [19,48] rather than by binding to the preexisting ice surface. It also agrees with results of our previous simulations of unrestrained proteins near various faces of ice [12]. We found that, on average, protein molecules that were initially located near the second minimum (at about 1 nm) did not change their distance very much from the faces of the underlying ice block much during the simulations when oriented with their ice-binding surfaces towards the *basal* and *primary prism* crystallographic planes of ice.

All of the above observations may be excellently explained with the use of two-order-parameter theory of liquids, developed recently by Tanaka [23–26,49]. The model describes the properties of liquids that are created by molecules that interact in a space-oriented manner. As a consequence, ordered, high volume structures are created in the liquid. Water is one of the representatives of this group of liquids. Some of the ordered structures that emerge in water are consistent with the geometry of hexagonal ice, such as six-membered rings and octameric units, while others are not – for example five-membered rings [49,50]. The presence of the latter counteracts the freezing and is responsible for the supercooling of the liquid and the phenomenon of glass transition. The model assumes that the ordered structures are present in small amount in abundance of disordered, high density structures formed by the remaining molecules of the liquid. Macroscopic properties of the liquid, such as density, compressibility, viscosity are governed by this equilibrium. Previously, we used some concepts from this model to explain density changes in solvation water of proteins [51].

We are now interested in the influence of the presence of the *Cf*AFP on the properties of interfacial water between the protein and the ice, as well as on the crystallization process. Because of that, the Tanaka model is, in our opinion, appropriate tool to apply to description of our system and the interpretation of the results. Consequently, we assume that in solvation water between the ice and the protein an equilibrium attempts to set between the ordered and disordered structures. We also assume that the equilibrium can be shifted by affecting the distance between the ice and the protein. Below we show that these assumptions are justified.

Typically in protein solvation shells the creation of the ordered structures may be hampered, leading to the increase in density of water [51]. In solvation water of ice, on the other hand, the formation of these structures is more probable (where the lattice of ice serves as a template). In solvation water of *Cf*AFP molecule (near its ice-binding plane), we also previously observed a tendency to create an ordered lattice, including rings formed by hydrogen-bonded water molecules [12]. Although it was not the same structurally and in degree of ordering as the one created at the ice surface, we postulated that it was similar enough to enable the merging of the two solvation shells. As a result, a larger conglomerate can be created, extending from the ice to the protein.

In attempt to characterize the degree of ordering of these conglomerates, we decided to analyze the presence of (strained) four-membered and (relaxed) five and six-membered rings in solvation

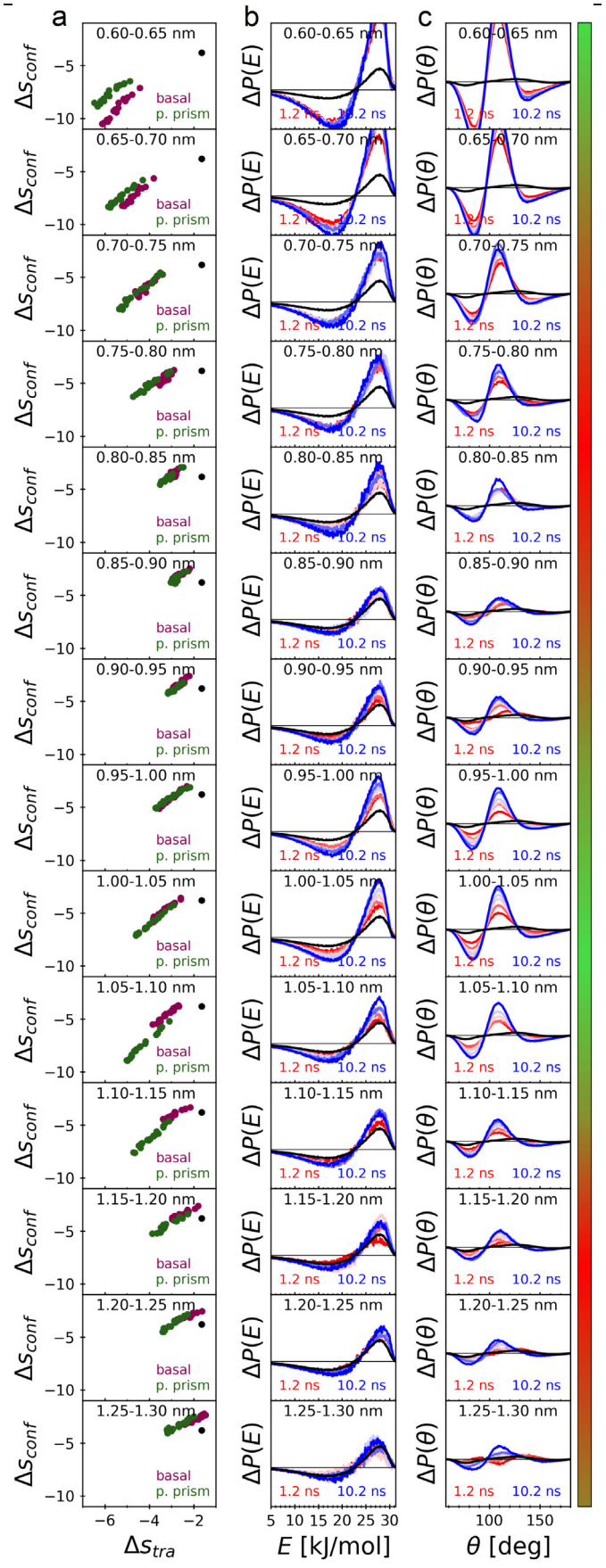

water of the protein. The number of these rings (divided by the number of water molecules in the solvation water) is presented in Fig. 4a. The temporal changes of the contents of the rings in solvation shell reflect the progress of the crystallization. During this process six-membered rings are created in increasing amount. As expected, the highest rate of changes in the number of the six-membered rings can be observed when the distance from the ice is close to the one corresponding to the minima in the free energy. When it comes to the five-membered rings, their geometry does not agree with the geometry of ice. The number of these rings changes slowly. This may reflect the fact that solvation water of *Cf*AFP, although similar to solvation water of ice in some regards [15–20], is not identical to it.

When the water crystallizes, the six-membered rings must be oriented in a specific manner relatively to the ice surface (as well as to the protein). Therefore, we also determined average orientation of rings relatively to the ice-binding surface of the *Cf*AFP molecule. The analysis of the histograms of the angles between the vectors normal to a plane fitted to the coordinates of water molecules creating these rings and the vector approximately perpendicular to the ice-binding surface of the protein molecule (linking the atoms C of THR 36 and CA of GLY 44, see Fig. S1) also reveals differences between the behavior of systems with the protein at the optimal distances and far from them. At the optimal distances, we observe high, distinct peaks for small values of the angles, while when the distance is far from optimal, the rings, if created, arrange themselves in a more chaotic way (Fig. 4c). This indicate that the rings arrange themselves relatively to the protein surface in a more parallel manner than they would if the solvation shell was filled with water which structure is bulk-like. Moreover, at non-optimal distances the rings themselves can become more distorted. As a measure of distortion, we can calculate the mean distance of the oxygen atoms from the center of the ring and then the standard deviation of the positions of oxygen atoms from this mean distance. We are aware that in some cases this parameter will give non-zero values even for ideal rings – one of the examples may be a boat conformation of six-membered ring. Since we are interested in the differences between properties of the solvation water and bulk liquid, we can nevertheless use it as an approximate measure of the distortion of the structure of rings in the vicinity of the protein. In the Fig. 4b we can see that these distortions are smallest for the distances close to these corresponding to the minima of the free energy.

Thanks to the measurements of the properties of the water rings, we can also observe some differences between the behavior of water when the protein is placed next to the *basal* plane and *primary prism* plane. Although the average orientation of the six-membered water rings relatively to the protein is similar, in the Supporting Information (Fig. S2), we described the results regarding an estimated percentage of the chair conformation of the six-membered rings – also revealing

Fig. 3. Selected structural properties of the solvation shell of the ice-binding surface of the *Cf*AFP molecule next to the *basal* and *primary prism* planes of ice. a) The ordering maps created with the use of the local ordering parameters (in J/(mol·K), differences with regard to bulk water – description in the text). The points (purple for *basal* and green for *primary prism* planes of ice) represent temporal changes of the parameters during the simulation (12 ns) – the values of both s_{tra} and s_{conf} become more negative as simulation progresses. The black point represents the ordering of the solvation water of the ice-binding surface of the *Cf*AFP molecule when it is not facing the ice. b) The distributions of the energies of the hydrogen bonds (differences with regard to bulk water). c) The distributions of the angles measured between vectors connecting a central water molecule with its hydrogen-bonded neighbors (differences with regard to bulk water). The protein-ice distance is indicated on each plot. Results presented in the Fig. 3b and c consider the proteins located next to the *basal* plane of ice. Results obtained in the case of the proteins located next to the *primary prism* plane of ice are qualitatively the same. The red-blue color scale in the Fig. 3b and c illustrates changes in time (red line corresponds to the time 1.2 ns from the start of the simulation, while the darkest blue line – at the end of the simulation; time interval between plots is constant and equal to 1.8 ns). Black lines in the Fig. 3b and c represents the results obtained for the ice-binding plane of protein when the ice crystal is not present in its vicinity. The red-green color bar placed on the right side of the figure indicates the approximate locations of the minima and maxima of the energy profile.

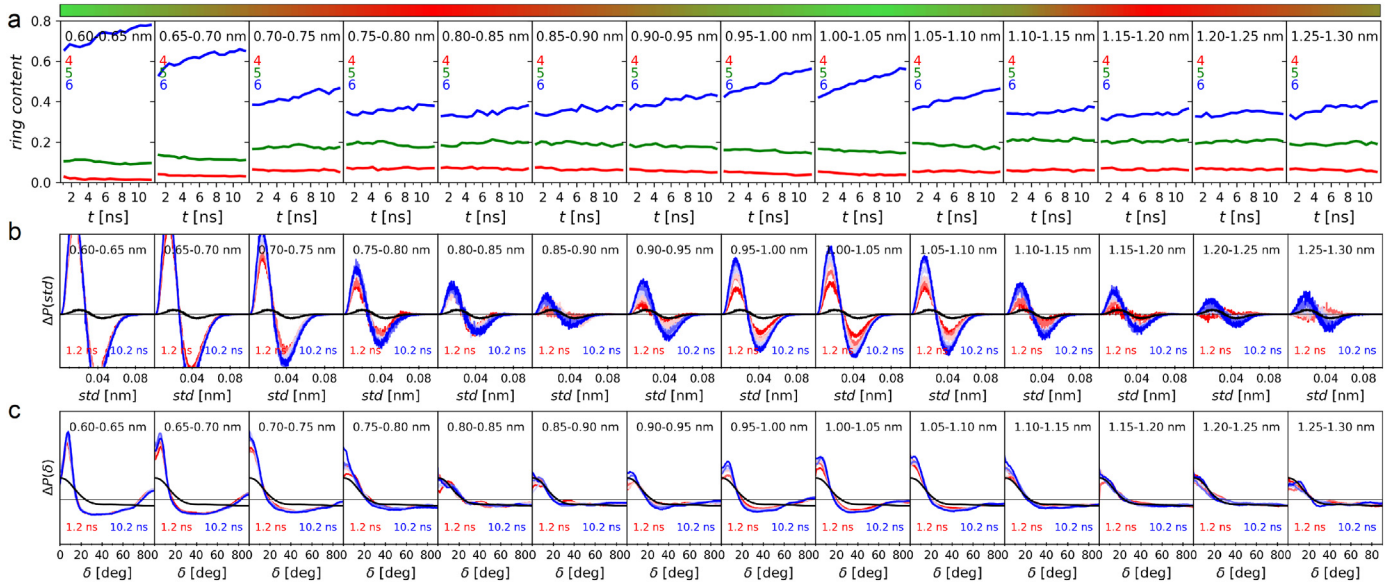

Fig. 4. a) The temporal changes in the number of the 4, 5 and 6-membered rings in the solvation shell of the ice-binding surface of the *Cf*AFP molecule next to the *basal* plane of ice (results are divided by the number of water molecules in the shell). b) The histograms of the standard deviations of the coordinates of the oxygen atoms of water molecules creating a six-membered water ring from the mean distance of these oxygen atoms from the center of the ring (differences with regard to bulk water). Results are presented for the proteins located next to the *basal* plane of ice. c) The histograms of the angles δ between two vectors: 1. the normal to the plane of the 6-membered water rings in solvation shell of the ice-binding surface of the *Cf*AFP molecule and 2. the vector running through the atoms C of THR 36 and CA of GLY 44 (approximately perpendicular to the ice-binding plane, see Fig. S1); next to the *basal* plane of ice (differences with regard to bulk water). The protein-ice distance is indicated on each plot. In all of the cases results obtained for the proteins located next to the *primary prism* plane of ice are qualitatively the same. The red-blue color scale in the Fig. 4b and c illustrates changes in time (the darkest red line correspond to the time 1.2 ns from the start of the simulation, while the darkest blue line – at the end of the simulation; time interval between plots is constant and equal to 1.8 ns). Black lines in the Fig. 4b and c represents the results obtained for the ice-binding plane of protein when the ice crystal is not present in its vicinity. The red-green color bar placed on top of the figure indicates the approximate locations of the minima and maxima of the energy profile.

differences between the two planes of ice. It is known that the mechanism of crystallization at the *basal* and *primary prism* is different [32,37,38,52]. The crystallization at the *basal* plane of hexagonal ice is slower and can result in creation of hexagonal or cubic layer of ice. At the *primary prism* plane, the crystallization is faster and leads to hexagonal ice only. In our simulations we did not observe the full adsorption of the protein onto the ice, therefore we do not have the data to characterize the interface at the basal and primary prism planes when the protein if fully frozen onto the ice. However, it was not necessary to analyze this interface because such analysis has already been performed by other authors, who found that in the adsorbed state, there are differences between the arrangement of the molecules in ice right under the AFP molecule when *basal* and *primary prism* planes are concerned [27].

Overall, our previous [12,22] and present analysis of the structure of water suggest that in the proximity of the protein surface water indeed arranges itself in a way that may evoke the anchored clathrate concept discussed in the introduction, because it can be turned into ice in right conditions. However, we should rather call it a "fluent clathrate" because prior to the crystallization the clathrate is by no means as sharply defined as in hydrated crystalline state [9]. It is not a regular, stable, ice-like structure. It should be viewed in terms of increased (or decreased) probability of certain arrangements of water molecules to occur, what can enable the smooth binding with ice, as we discussed previously [12,53].

In our results presented above, we can see the evidence for creation of the ordered structures in the *Cf*AFP-ice interfacial water when two solvation shells are merged. However, the prerequisite that needs to be met for these conglomerates to be created is a proper distance and orientation between the two associating surfaces. Alternatively, the aggregates are going to be deformed from their natural shape (squeezed or stretched) or even destroyed. As a consequence, when the *Cf*AFP molecule is not optimally placed, the force emerges that pushes it away from the surface of ice or pulls it closer towards it, facilitating the creation of these structures and hence also the later adsorption.

4. Conclusions

The concept that in liquid water some ordered, high-volume structures can be created in abundance of low-volume, disordered structures was used to explain many unusual properties of water [49]. We postulate that in liquid water between the *Cf*AFP molecule and the ice surface, high-volume, ordered aggregates can emerge in number higher than in bulk water. At the ice surface, they can be built on the existing ice lattice. In the solvation water of an ice-binding surface of *Cf*AFP, these aggregates can also be created. Nearest to the protein, a kind of a "fluent clathrate" is created that is not a sharply defined, crystal-like structure as found by Garnham et al. in solid state and called anchored clathrate. It is plastic, changes its structure during crystallization and is able to match different crystallographic planes of ice. The aggregates near the ice can merge with the solvation water of *Cf*AFP, when the protein comes close enough to the ice. The final structure of this merged aggregate depends on the distance between the ice and the approaching protein. If this distance is optimal, then the aggregate can be formed in its proper structure. However, when the distance is not optimal, the resulting aggregate will be deformed (squeezed or stretched, or even destroyed). As a result, a force is exerted on the *Cf*AFP molecule (pushing it away from the ice or pulling closer towards the ice), aiming to correct the positioning. When the distance is optimal, corresponding to the minimum of the free energy, the aggregates are going to solidify, biding the protein to the ice. This model of interactions between two surfaces, mediated by interfacial water, can be applied, in our opinion, to variety of systems, including, for example, two interacting *Ri*AFP molecules [36].

CRediT authorship contribution statement

Joanna Grabowska: Writing - review & editing, Investigation, Software, Methodology, Funding acquisition. **Anna Kuffel:** Writing - review & editing, Investigation, Software, Methodology. **Jan Zielkiewicz:**

Writing - original draft, Writing - review & editing, Investigation, Software, Methodology.

Declaration of competing interest

The authors declare that they have no known competing financial interests or personal relationships that could have appeared to influence the work reported in this paper.

Acknowledgments

J.G. acknowledges support from National Science Centre, Poland, grant no. 2017/27/N/ST4/02519. The calculations were carried out at the Academic Computer Center (TASK) in Gdańsk. This research was supported in part by PL-Grid Infrastructure.

Appendix A. Supplementary data

Supplementary data to this article can be found online at https://doi.org/10.1016/j.molliq.2020.112909.

References

[1] A.J. Scotter, C.B. Marshall, L.A. Graham, J.A. Gilbert, C.P. Garnham, P.L. Davies, The basis for hyperactivity of antifreeze proteins, Cryobiology 53 (2006) 229–239, https://doi.org/10.1016/j.cryobiol.2006.06.006.
[2] Y. Celik, R. Drori, N. Pertaya-Braun, A. Altan, T. Barton, M. Bar-Dolev, A. Groisman, P.L. Davies, I. Braslavsky, Microfluidic experiments reveal that antifreeze proteins bound to ice crystals suffice to prevent their growth, Proc. Natl. Acad. Sci. 110 (2013) 1309–1314, https://doi.org/10.1073/pnas.1213603110.
[3] N. Pertaya, C.B. Marshall, C.L. DiPrinzio, L. Wilen, E.S. Thomson, J.S. Wettlaufer, P.L. Davies, I. Braslavsky, Fluorescence microscopy evidence for quasi-permanent attachment of antifreeze proteins to ice surfaces, Biophys. J. 92 (2007) 3663–3673, https://doi.org/10.1529/biophysj.106.096297.
[4] O.A. Karim, A.D.J. Haymet, The ice/water interface: a molecular dynamics simulation study, J. Chem. Phys. 89 (1988) 6889–6896, https://doi.org/10.1063/1.455363.
[5] D. Beaglehole, P. Wilson, Thickness and anisotropy of the ice-water interface, J. Phys. Chem. 97 (1993) 11053–11055, https://doi.org/10.1021/j100144a025.
[6] M.M. Conde, C. Vega, A. Patrykiejew, The thickness of a liquid layer on the free surface of ice as obtained from computer simulation, J. Chem. Phys. 129 (2008) https://doi.org/10.1063/1.2940195.
[7] K.A. Sharp, A peek at ice binding by antifreeze proteins, Proc. Natl. Acad. Sci. 108 (2011) 7281–7282, https://doi.org/10.1073/pnas.1104618108.
[8] A. Wierzbicki, P. Dalal, T.E. Cheatham, J.E. Knickelbein, A.D.J. Haymet, J.D. Madura, Antifreeze proteins at the ice/water interface: three calculated discriminating properties for orientation of type I proteins, Biophys. J. 93 (2007) 1442–1451, https://doi.org/10.1529/biophysj.107.105189.
[9] C.P. Garnham, R.L. Campbell, P.L. Davies, Anchored clathrate waters bind antifreeze proteins to ice, Proc. Natl. Acad. Sci. 108 (2011) 7363–7367, https://doi.org/10.1073/pnas.1100429108.
[10] A. Hakim, J.B. Nguyen, K. Basu, D.F. Zhu, D. Thakral, P.L. Davies, F.J. Isaacs, Y. Modis, W. Meng, Crystal structure of an insect antifreeze protein and its implications for ice binding, J. Biol. Chem. 288 (2013) 12295–12304, https://doi.org/10.1074/jbc.M113.450973.
[11] S. Chakraborty, B. Jana, Molecular insight into the adsorption of spruce budworm antifreeze protein to an ice surface: a clathrate-mediated recognition mechanism, Langmuir 33 (2017) 7202–7214, https://doi.org/10.1021/acs.langmuir.7b01733.
[12] J. Grabowska, A. Kuffel, J. Zielkiewicz, Molecular dynamics study on the role of solvation water in the adsorption of hyperactive AFP to the ice surface, Phys. Chem. Chem. Phys. 20 (2018) 25365–25376, https://doi.org/10.1039/C8CP05027A.
[13] S. Chakraborty, B. Jana, Conformational and hydration properties modulate ice recognition by type I antifreeze protein and its mutants, Phys. Chem. Chem. Phys. 19 (2017) 11678–11689, https://doi.org/10.1039/C7CP00221A.
[14] K. Meister, S. Strazdaite, A.L. DeVries, S. Lotze, L.L.C. Olijve, I.K. Voets, H.J. Bakker, M.L. Klein, Observation of ice-like water layers at an aqueous protein surface, Proc. Natl. Acad. Sci. 111 (2014) 17732–17736, https://doi.org/10.1073/pnas.1414188111.
[15] K.R. Gallagher, K.A. Sharp, Analysis of thermal hysteresis protein hydration using the random network model, Biophys. Chem. 105 (2003) 195–209, https://doi.org/10.1016/S0301-4622(03)00087-5.
[16] C. Yang, K.A. Sharp, The mechanism of the type III antifreeze protein action: a computational study, Biophys. Chem. 109 (2004) 137–148, https://doi.org/10.1016/j.bpc.2003.10.024.
[17] N. Smolin, V. Daggett, Formation of ice-like water structure on the surface of an antifreeze protein, J. Phys. Chem. B 112 (2008) 6193–6202, https://doi.org/10.1021/jp710546e.
[18] C. Yang, K.A. Sharp, Hydrophobic tendency of polar group hydration as a major force in type I antifreeze protein recognition, Proteins Struct. Funct. Bioinforma. 59 (2005) 266–274, https://doi.org/10.1002/prot.20429.
[19] D.R. Nutt, J.C. Smith, Dual function of the hydration layer around an antifreeze protein revealed by atomistic molecular dynamics simulations, J. Am. Chem. Soc. 130 (2008) 13066–13073, https://doi.org/10.1021/ja8034027.
[20] A. Kuffel, D. Czapiewski, J. Zielkiewicz, Unusual structural properties of water within the hydration shell of hyperactive antifreeze protein, J. Chem. Phys. 141 (2014), 055103. https://doi.org/10.1063/1.4891810.
[21] A. Hudait, D.R. Moberg, Y. Qiu, N. Odendahl, F. Paesani, V. Molinero, Preordering of water is not needed for ice recognition by hyperactive antifreeze proteins, Proc. Natl. Acad. Sci. 115 (2018) 8266–8271, https://doi.org/10.1073/pnas.1806996115.
[22] J. Grabowska, A. Kuffel, J. Zielkiewicz, Role of the solvation water in remote interactions of hyperactive antifreeze proteins with the surface of ice, J. Phys. Chem. B 123 (2019) 8010–8018, https://doi.org/10.1021/acs.jpcb.9b05664.
[23] H. Tanaka, Simple physical explanation of the unusual thermodynamic behavior of liquid water, Phys. Rev. Lett. 80 (1998) 5750–5753, https://doi.org/10.1103/PhysRevLett.80.5750.
[24] H. Tanaka, Two-order-parameter description of liquids. I. a general model of glass transition covering its strong to fragile limit, J. Chem. Phys. 111 (1999) 3163–3174, https://doi.org/10.1063/1.479596.
[25] H. Tanaka, Simple physical model of liquid water, J. Chem. Phys. 112 (2000) 799–809, https://doi.org/10.1063/1.480609.
[26] J. Russo, H. Tanaka, Understanding water's anomalies with locally favoured structures, Nat. Commun. 5 (2014) 3556, https://doi.org/10.1038/ncomms4556.
[27] A. Hudait, N. Odendahl, Y. Qiu, F. Paesani, V. Molinero, Ice-nucleating and antifreeze proteins recognize ice through a diversity of anchored clathrate and ice-like motifs, J. Am. Chem. Soc. 140 (2018) 4905–4912, https://doi.org/10.1021/jacs.8b01246.
[28] D.A. Case, T.A. Darden, T.E. Cheatham III, C.L. Simmerling, J. Wang, R.E. Duke, R. Luo, R.C. Walker, W. Zhang, K.M. Merz, B. Roberts, S. Hayik, A. Roitber, G. Seabra, J. Swails, A.W. Götz, I. Kolossváry, K.F. Wong, F. Paesani, J. Vanicek, R.M. Wolf, J. Liu, X. Wu, S.R. Brozell, T. Steinbrecher, H. Gohlke, Q. Cai, X. Ye, J. Wang, M.-J. Hsieh, G. Cui, D.R. Roe, D.H. Mathews, M.G. Seetin, R. Salomon-Ferrer, C. Sagui, V. Babin, T. Luchko, S. Gusarov, A. Kovalenko, P.A. Kollman, Amber 12. Reference Manual, University of California, San Francisco, 2012.
[29] Y. Duan, C. Wu, S. Chowdhury, M.C. Lee, G. Xiong, W. Zhang, R. Yang, P. Cieplak, R. Luo, T. Lee, J. Caldwell, J. Wang, P. Kollman, A point-charge force field for molecular mechanics simulations of proteins based on condensed-phase quantum mechanical calculations, J. Comput. Chem. 24 (2003) 1999–2012, https://doi.org/10.1002/jcc.10349.
[30] J.L.F. Abascal, E. Sanz, R. García Fernández, C. Vega, A potential model for the study of ices and amorphous water: TIP4P/ice, J. Chem. Phys. 122 (2005), 234511. https://doi.org/10.1063/1.1931662.
[31] E.K. Leinala, P.L. Davies, Z. Jia, Crystal structure of β-helical antifreeze protein points to a general ice binding model, Structure 10 (2002) 619–627, https://doi.org/10.1016/S0969-2126(02)00745-1.
[32] J. Grabowska, A. Kuffel, J. Zielkiewicz, The accretion of the new ice layer on the surface of hexagonal ice crystal and the influence of the local electric field on this process, J. Chem. Phys. 147 (2017), 174502. https://doi.org/10.1063/1.4994612.
[33] Schrödinger, The PyMOL Molecular Graphics System, Version 2.1, LCC. (n.d.).
[34] W. Hwang, M.J. Lang, M. Karplus, Force generation in kinesin hinges on cover-neck bundle formation, Structure 16 (2008) 62–71, https://doi.org/10.1016/j.str.2007.11.008.
[35] A. Kuffel, M. Szałachowska, The significance of the properties of water for the working cycle of the kinesin molecular motor, J. Chem. Phys. 148 (2018), 235101. https://doi.org/10.1063/1.5020208.
[36] K. Mochizuki, M. Matsumoto, Collective transformation of water between hyperactive antifreeze proteins: RiAFPs, Crystals 9 (2019) 188, https://doi.org/10.3390/cryst9040188.
[37] H. Nada, Y. Furukawa, Anisotropy in growth kinetics at interfaces between proton-disordered hexagonal ice and water: a molecular dynamics study using the six-site model of H_2O, J. Cryst. Growth 283 (2005) 242–256, https://doi.org/10.1016/j.jcrysgro.2005.05.057.
[38] M.A. Carignano, P.B. Shepson, I. Szleifer, Molecular dynamics simulations of ice growth from supercooled water, Mol. Phys. 103 (2005) 2957–2967, https://doi.org/10.1080/00268970500243796.
[39] P.-L. Chau, A.J. Hardwick, A new order parameter for tetrahedral configurations, Mol. Phys. 93 (1998) 511–518, https://doi.org/10.1080/002689798169195.
[40] E. Shiratani, M. Sasai, Molecular scale precursor of the liquid–liquid phase transition of water, J. Chem. Phys. 108 (1998) 3264–3276, https://doi.org/10.1063/1.475723.
[41] E. Shiratani, M. Sasai, Growth and collapse of structural patterns in the hydrogen bond network in liquid water, J. Chem. Phys. 104 (1996) 7671–7680, https://doi.org/10.1063/1.471475.
[42] P.J. Steinhardt, D.R. Nelson, M. Ronchetti, Bond-orientational order in liquids and glasses, Phys. Rev. B 28 (1983) 784–805, https://doi.org/10.1103/PhysRevB.28.784.
[43] A.H. Nguyen, V. Molinero, Identification of clathrate hydrates, hexagonal ice, cubic ice, and liquid water in simulations: the CHILL+ algorithm, J. Phys. Chem. B 119 (2015) 9369–9376, https://doi.org/10.1021/jp510289t.
[44] E. Duboué-Dijon, D. Laage, Characterization of the local structure in liquid water by various order parameters, J. Phys. Chem. B 119 (2015) 8406–8418, https://doi.org/10.1021/acs.jpcb.5b02936.
[45] J. Grabowska, A. Kuffel, J. Zielkiewicz, Structure of solvation water around the active and inactive regions of a type III antifreeze protein and its mutants of lowered activity, J. Chem. Phys. 145 (2016), 075101. https://doi.org/10.1063/1.4961094.
[46] T.M. Truskett, S. Torquato, P.G. Debenedetti, Towards a quantification of disorder in materials: distinguishing equilibrium and glassy sphere packings, Phys. Rev. E 62 (2000) 993–1001, https://doi.org/10.1103/PhysRevE.62.993.
[47] R. Esposito, F. Saija, A. Marco Saitta, P.V. Giaquinta, Entropy-based measure of structural order in water, Phys. Rev. E 73 (2006), 040502. https://doi.org/10.1103/PhysRevE.73.040502.

[48] E. Kristiansen, K.E. Zachariassen, The mechanism by which fish antifreeze proteins cause thermal hysteresis, Cryobiology 51 (2005) 262–280, https://doi.org/10.1016/j.cryobiol.2005.07.007.
[49] H. Tanaka, Thermodynamic anomaly and polyamorphism of water, Europhys. Lett. 50 (2000) 340–346, https://doi.org/10.1209/epl/i2000-00276-4.
[50] F.H. Stillinger, Water revisited, Science (80-.) 209 (1980) 451–457, https://doi.org/10.1126/science.209.4455.451.
[51] A. Kuffel, J. Zielkiewicz, Why the solvation water around proteins is more dense than bulk water, J. Phys. Chem. B 116 (2012) 12113–12124, https://doi.org/10.1021/jp305172t.
[52] M. Seo, E. Jang, K. Kim, S. Choi, J.S. Kim, Understanding anisotropic growth behavior of hexagonal ice on a molecular scale: a molecular dynamics simulation study, J. Chem. Phys. 137 (2012), 154503. https://doi.org/10.1063/1.4759113.
[53] S. Chakraborty, B. Jana, Optimum number of anchored clathrate water and its instantaneous fluctuations dictate ice plane recognition specificities of insect antifreeze protein, J. Phys. Chem. B 122 (2018) 3056–3067, https://doi.org/10.1021/acs.jpcb.8b00548.